

Article

Awaruite, a New Large Nickel Resource: Flotation under Weakly Acidic Conditions

Santiago Seiler ^{1,2,*} , Gustavo Sánchez ² , Marek Pawlik ¹, Peter Bradshaw ³ and Bern Klein ¹

¹ Norman B. Keevil Institute of Mining Engineering, Faculty of Applied Science, University of British Columbia, 517-6350 Stores Road, Vancouver, BC V6T 1Z4, Canada

² Departamento Ingeniería de Materiales y Minas, Facultad de Ingeniería, Universidad de la República, Julio Herrera y Reissig 565, Montevideo CP 11300, Uruguay

³ FPX Nickel Corporation, 320-1155 West Pender Street, Vancouver, BC V6E 2P4, Canada

* Correspondence: sseiler@alumni.ubc.ca

Abstract: To support the transformation to clean low carbon technologies, there is a demand for critical metals such as nickel. Awaruite is a less common nickel-bearing mineral with unique properties and responses to mineral separation. This paper presents the findings of a flotation study to recover awaruite from the Baptiste ultramafic deposit, located in central British Columbia, Canada. Nickel recoveries of up to 65% at the rougher stage were obtained with xanthate as a collector at a pH level of 4.5. Awaruite flotation was shown to be highly dependent on the slurry pH. At weakly acidic conditions, the awaruite surface is activated through the dissolution of the passivation layer formed during grinding in alkaline conditions. Desliming was shown to reduce the acid consumption required to maintain the pH, probably by removing the highly reactive serpentine slimes generated during grinding. Rougher, followed by cleaner stages of flotation, showed that a high-grade concentrate can be produced with up to 45% nickel, 1.3% cobalt, 0.7% copper and negligible concentrations of penalty elements, such as arsenic, lead, and selenium, among others. A nickel flotation concentrate from an awaruite deposit is a promising feedstock for not only stainless-steel production but also for clean energy technologies.

Keywords: awaruite; nickel; flotation; serpentine; desliming



Citation: Seiler, S.; Sánchez, G.; Pawlik, M.; Bradshaw, P.; Klein, B. Awaruite, a New Large Nickel Resource: Flotation under Weakly Acidic Conditions. *Minerals* **2023**, *13*, 1147. <https://doi.org/10.3390/min13091147>

Academic Editors: Feridun Boylu, Orhan Özdemir and Onur Guven

Received: 24 July 2023

Revised: 24 August 2023

Accepted: 28 August 2023

Published: 30 August 2023



Copyright: © 2023 by the authors. Licensee MDPI, Basel, Switzerland. This article is an open access article distributed under the terms and conditions of the Creative Commons Attribution (CC BY) license (<https://creativecommons.org/licenses/by/4.0/>).

1. Introduction

Nickel has outstanding physical and chemical properties, which make it essential in many products. Its main application is in alloying, particularly when producing stainless and heat-resistant steels with chromium and other metals. There are two types of primary nickel products: high-purity Class 1 products (containing 99.8% nickel or above) and lower-purity Class 2 products (containing less than 99.8% nickel). Class 1 products are crucial for the development of clean energy technologies since it is used as cathode material for batteries or in the form of alloys for renewable energies and hydrogen. The demand for nickel is projected to grow by around 19 times from 2020 to 2040 [1].

The nickel resources are classified into two types: sulfides and laterites. In general, nickel sulfide ores are mined to supply Class 1 products since the concentrating and refining process is cheaper than lateritic ores (oxide resources) [1,2]. Most of the production growth in the future is expected to come from lateritic ores and not from sulfide ores. A deficit in the nickel supply for Class 1 products is expected in the medium term, thus increasing the interest on nickel deposits capable of producing Class 1 products using less energy-intensive methods than those that are currently used for lateritic ores [3].

The Baptiste deposit, located in central British Columbia, Canada, hosts a nickel mineralization where most of the nickel occurs as awaruite [4]. Awaruite (Ni₃Fe) is an intermetallic compound of nickel and iron [5]. It has high density (8.6 g/cm³) and magnetic susceptibility ($\chi = 14.4$) [6]. In the Baptiste deposit, awaruite has an average composition of 77.3% nickel,

21.0% iron, 1.1% cobalt, and 0.6% copper [6]. Occurrences of awaruite have been mainly related to serpentized ultramafic rocks, which is the case for the Baptiste deposit [7,8].

The main gangue material in the Baptiste deposit is serpentine [7]. Serpentine is a group of minerals, including lizardite, antigorite, and chrysotile [9]. They all have the same ideal composition, $Mg_3Si_2O_5(OH)_4$, but vary significantly in their crystal structure. The serpentine minerals are made of a layer of magnesium hydroxide, commonly referred to as the 'brucite' layer, stacked on a layer of silica [10].

The layered structure of serpentine, along with its low hardness, makes it prone to over-grinding in mineral processing operations, which is reflected by the formation of slimes (fine to ultrafine particles). Serpentine slimes have a deleterious effect on sulfide mineral flotation [11,12]. Desliming is applied to reduce the deleterious effect of slimes [13–15]. Since slimes are composed of predominantly serpentine gangue minerals, the best technical option to deal with the issue is to eliminate the slimes prior to flotation. The addition of acid has also been proposed to minimize the effect of slimes [12,16]. The brucite layer that forms the serpentine structure is readily soluble at neutral and acidic conditions; thus, serpentine partially dissolves, leaving the silica layer with a porous structure. High acid addition is required to have a meaningful impact on the flotation performance when slimes are present [12]. Desliming is recommended to remove the slimes and to minimize the acid consumption.

The available information concerning the recovery and concentration of awaruite is scarce. Magnetic and gravity separation have been the focus of published work, along with whole ore leaching [17–19]. Magnetic separation has been shown to efficiently concentrate awaruite but not in a selective way since magnetite is recovered together with awaruite [20]. Flotation has been proposed to separate awaruite from magnetite [4,15]. However, limited information is available on the flotation conditions required to effectively concentrate awaruite. Single mineral experiments performed by the authors of this manuscript showed that awaruite readily floats in acidic conditions in the presence of xanthate [21]. The surface of awaruite passivates under neutral and alkaline conditions, thus impeding the interaction between the xanthate collector and the metallic phase. Under acidic conditions, the oxide coating is dissolved, exposing the metallic phase and thereby activating the interaction between the surface and the collector [21].

The single mineral experimental results are aligned with metallurgical studies on magnetic concentrates, which have demonstrated the awaruite floatability in such conditions [4]. Nevertheless, there is no detailed study of the effect of pH conditioning on the flotation of awaruite in fresh rock samples containing serpentine without pre-concentration. To the best of the authors' knowledge, this work is the first to investigate awaruite flotation at bench scale at acidic conditions with actual rock samples. The understanding of the effect of pH on the flotation of awaruite in the presence of serpentine minerals is fundamentally important to the development of a reliable mineral processing flowsheet to recover awaruite.

The present paper builds off previous work performed by the authors on pure awaruite samples that demonstrated that acid addition can remove an oxidation layer from awaruite, allowing flotation with xanthate collectors. The goal is to identify conditions that allow the achievement of high Ni recoveries and high-grade products through stages of rougher and cleaner flotation for industrial practice. The main objective of the present study is to assess the effect of acid addition on awaruite flotation in the presence of gangue minerals and, specifically, serpentine. The study also assesses the "optimum" pH level, the impacts of desliming on acid consumption, and the effect of cleaning flotation on concentrate grade.

2. Materials and Methods

2.1. Material

The raw material used in this work originated from the Baptiste deposit (FPX Nickel Corp., Vancouver, BC, Canada) located in central British Columbia, Canada. The material was provided as pieces of drill core representing the proposed life of mine mill feed and the variations of mineralization present in the deposit.

2.2. Material Preparation and Analysis

The sample preparation before grinding included mixing, crushing to -6 mesh (3.35 mm), and riffle splitting into 1 kg subsamples. Grinding was then performed in a lab-scale rod mill at 60 wt.% solids to prepare samples for flotation testing. The ground ore was either sent straight to flotation or deslimed using a 51 mm diameter Mozley cyclone (See Figure S1 for equipment photo and Table S1 for operating parameters). The whole and deslimed samples were subjected to automated mineralogical analysis using QEMSCAN[®] and to wet chemical assay.

2.3. Bench Flotation

Flotation tests were carried out using a Denver D12 lab-scale flotation cell operated at 1200 rpm with a constant airflow of 5 L/min. The suspensions were mixed for 1 min, and then the pH was adjusted by adding diluted 0.5 or 1 M sulfuric acid. The sulfuric acid was of analytical quality, and the solutions were prepared with distilled water. The pH was monitored continuously and maintained automatically. The oxidation-reduction potential was also monitored and recorded with the same controller. A photo of the setup was added to the Supplementary Material, Figure S2.

For the rougher flotation tests, the collector was added to the cell after 10 min of conditioning at stable pH values, and the suspension with the collector was allowed to condition for 2 min. The conditioning time was selected based on a previous work carried out by the authors [21]. After collector conditioning time, the frother was added, and the suspension was conditioned for 1 min more before starting the collection of the first concentrate. A total of four concentrates were collected with pulp level re-adjustment in between each of them, along with the collector and frother additions in an identical regimen to the one described for the first concentrate collection (Figure 1). Each of the four concentrates was collected during 2 min. For the rougher-cleaner flotation, three cleaning steps were applied to increase the final product grade (Figure 1). Details about regrinding and particle size distribution of the reground material are presented in the Supplementary Material. The flotation products were filtered, dried, and analyzed for the elements of interest: Ni, Fe, and S. Duplicate tests were carried out to ensure repeatability.

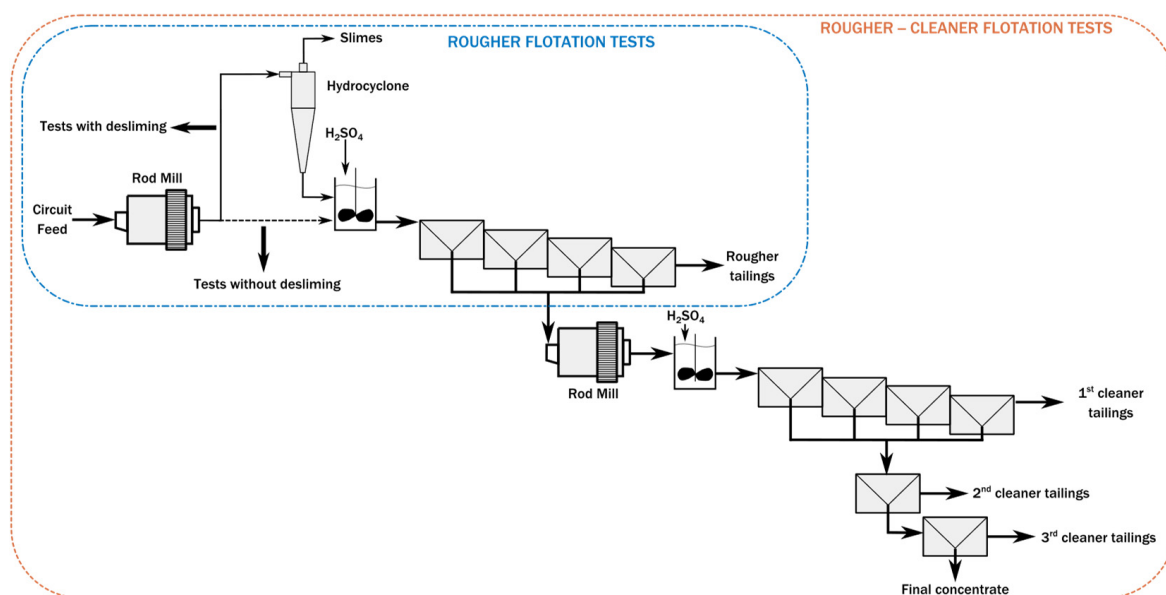


Figure 1. Rougher and rougher-cleaner flotation flowsheets with and without desliming.

In all flotation tests, the collector reagent used was potassium amyl xanthate ($\text{KC}_6\text{H}_{11}\text{OS}_2$) of industrial grade. The collector was kept in petroleum ether in the fridge, and fresh solutions were prepared daily. Fresh collector was added in all the flotation stages to overcome the

losses due to decomposition in an acidic solution [22]. A total collector dosage of 140 g/ton of flotation feed was used in the rougher stages and 20 g/ton in the cleaner flotation tests. A poly glycol ether (DOWFROTH™ 200) was used as a flotation frother with dosages of 100 g/ton in the rougher stage and 50 g/ton in the cleaner tests.

3. Results and Discussion

3.1. Material Characteristics

Table 1 shows the head grade of the elements of interest: Ni, Fe, and S in the raw material (identified as Feed). Normalized distribution of mineral composition for the whole and deslimed samples, as obtained from QEMSCAN, is shown in Table 2. A more detailed mineralogical characterization of the material, including x-ray diffraction and chemical composition, is presented in a separate work of the same authors, carried out in a representative subsample [6]. In terms of particle size distribution, the P_{80} of the feed sample is 82 μm and has a considerable portion of fines; in all, 34 wt.% of the sample is below 20 μm . Figure S3a shows the particle size distribution of the feed sample after grinding, as well as that of the desliming products, overflow, and underflow. For the Baptiste sample, hydrocyclone desliming was shown to also be effective at removing slimes (Figure S3a). As a comparison, the fraction of sample below 20 μm in the underflow is 14 wt.%, and in the overflow is 90 wt.%. The mass split to underflow is 73.8%. The partition curve of the size separation process is shown in Figure S3b. The corrected cut-point is 17 μm , and the imperfection index is 0.26, which is within the expected range of values for this kind of separation [23].

Table 1. Metallurgical balance of the hydrocyclone desliming test.

Products	Mass [%]	Element Content [%]			Distribution [%]		
		Ni	Fe	S	Ni	Fe	S
Underflow (deslimed sample)	73.8	0.23	6.83	0.08	86.6	83.4	91.8
Overflow (slimes)	26.2	0.10	3.83	0.02	13.4	16.6	8.2
Feed	100.0	0.20	6.04	0.06	100.0	100.0	100.0

Table 2. Normalized distribution of mineral composition for the whole and deslimed samples as obtained from QEMSCAN.

Mineral	Whole Sample	Deslimed Sample
<i>nickel minerals</i>		
awaruite	0.31	0.32
nickel sulfides *	0.06	0.05
<i>gangue minerals</i>		
serpentine	85.2	77.2
olivine	4.69	12.3
pyroxene/amphibole	3.99	3.56
magnetite	2.84	3.00
chromite	0.94	1.30
brucite/magnesite-siderite	0.56	0.48
others	1.42	1.84

* Includes pentlandite, cobalt pentlandite, and heazlewoodite/millerite/polydymite.

The large content of fines can be explained by the rock type present in the Baptiste deposit. As shown in Table 2, serpentine is the most abundant mineral in the rock (85.2%), followed by olivine (4.7%), which is the unaltered mineral of the serpentinization process. The presence of olivine is an indication that the serpentinization process was not completed, and some of the original rock is still present. The presence of slimes for this rock type is reported in other similar mines and deposits, such as Mt Keith and the Dumont, Crawford, and Pipe deposits [12,14,15,24]. In all these cases, desliming has been suggested or implemented to remove the slimes or at least process the slimes separately from the coarser particles.

Desliming for the Baptiste sample was shown to selectively remove gangue minerals, mainly serpentine. The content of serpentine (Table 2) decreased from 85.2% in the whole sample to 77.2% in the deslimed sample, and as a result, the content of olivine increased from 4.7% in the whole sample to 12.3% in the deslimed sample. The selective separation can also be observed in Table 1. The nickel recovery to the underflow (deslimed sample) is 86.6%, and the nickel grade of the underflow is 0.23%, which is higher than the grade of the slimes (0.10%). Similar enrichment is observed for iron and sulfur, where the grade of the underflow is higher than the grade of the overflow.

In the Baptiste sample, nickel is mainly hosted as awaruite (89.5%) and the rest as nickel sulfides (Table 3). This nickel department is consistent with other studies carried out on samples from the Baptiste deposit. Awaruite forms in a reducing environment, at low sulfur and oxygen fugacities, during the breakdown of olivine or nickel-bearing sulfides and is commonly associated with Ni-rich sulfides [25]. For the Baptiste sample, the distribution of nickel sulfides between nickel-rich and nickel-poor is fairly even, and they represent roughly 10% of the nickel present in the sample. Nickel-poor includes pentlandite $[(\text{Ni},\text{Fe})_9\text{S}_8]$ and cobaltpentlandite $[(\text{Co},\text{Ni},\text{Fe})_9\text{S}_8]$, and nickel-rich includes heazlewoodite $[\text{Ni}_3\text{S}_2]$ and millerite $[\text{NiS}]$. The desliming process does not alter the nickel department; the fraction of nickel present as awaruite is similar between the whole sample and the deslimed sample (Table 3). Furthermore, the nickel department does not considerably change over different size fractions. However, the nickel department as sulfides is slightly higher in the finer fractions for both the whole and deslimed samples.

Table 3. Normalized distribution by size range of nickel minerals.

Whole Sample				
Size Fraction [μm]	Mass [%]	% Ni of Total Ni		
		Pe	Haz	Aw
>106	16	1.9	4.3	93.8
38–106	44	5.7	4.4	89.9
0–38	40	8.9	6.2	84.9
Total	100	5.7	4.8	89.5
Deslimed Sample				
Size Fraction [μm]	Mass [%]	% Ni of Total Ni		
		Pe	Haz	Aw
>75	30	2.6	2.8	94.6
38–75	37	2.6	6.8	90.6
0–38	33	5.9	13.8	80.3
Total	100	3.4	6.6	90.0

Note: Pe-Pentlandite/Cobalt Pentlandite, Haz-Heazlewoodite/Millerite/Polydymite, Aw-Awaruite.

Awaruite in the Baptiste sample is found in fairly fine particle size. The automated mineralogical analysis showed that 80% of the awaruite mineral grains are smaller than 27 μm and 50% are smaller than 9 μm . This particle size measurement is a rough estimation

due to the elongated shape factor generally observed in awaruite samples [6]. For the deslimed sample, the measured particle size distribution showed that 50% of the awaruite is smaller than 49 μm , and 80% is smaller than 90 μm . The difference in the particle size distribution between the whole and deslimed sample is an indication that in the desliming process, awaruite is lost as fine to ultrafine particles (<10 μm). A more detailed mineralogical characterization of the sample is available in another article published by the same authors [6].

3.2. Rougher Flotation

3.2.1. Nickel Recoveries

Table 4 shows the final nickel recovery and grade values for the rougher flotation tests at each pH value. The recoveries for each pH level show a strong dependence on the flotation performance with the pH. At pH 6.5, the nickel recovery is poor, and the enrichment ratio is low, i.e., the grade of the concentrate is fairly similar to the feed grade (Table 1). The flotation performance improves at lower pH levels such that at pH 5.5, the final nickel recovery increases considerably to about 50%.

Table 4. Final nickel recovery and grade values for the rougher flotation tests at each pH value.

Sample Description	Rougher Concentrate	Flotation pH				
		3.5	4.5	5	5.5	6.5
Whole	Final Ni recovery [%]	60.7	64.7	--	50.8	15.2
	Final Ni grade [%]	0.9	1.0	--	0.8	0.2
Deslimed	Final Ni recovery [%]	57.3	61.3	51.8	49.5	18.9
	Final Ni grade [%]	1.1	1.2	0.9	0.9	0.5

The largest change in flotation performance is observed when lowering the pH from 5.5 to 4.5. At pH 4.5, nickel recoveries of up to 64.7% and 61.3% with product grades of 1.0%–1.2% nickel were obtained for both the whole and deslimed samples, respectively. There is no considerable difference in the nickel recovery between pH 4.5 and 3.5. However, nickel grades and recoveries tend to be slightly higher at pH 4.5 than at pH 3.5, thus indicating that decreasing the pH from 4.5 to 3.5 does not lead to an improvement in the flotation performance.

Figure 2 shows the nickel grade vs. recovery (cumulative) for the flotation of the whole and deslimed samples at different pH levels. The four points of each curve correspond to the four concentrates sequentially collected in each test (1, 2, 3, and 4). As observed, the flotation pH not only affects the final concentrate recovery and grade but also the flotation kinetics. Recoveries higher than 50% are achieved after just 2 min of flotation. The faster kinetic implies a possible scale-up of the process in terms of a reduced residence time required to recover awaruite. These results support the selection of pH 4.5 as the suggested flotation condition.

In general, the nickel recoveries for the whole sample were higher than the recoveries of the deslimed sample at the same pH levels. A flotation test was performed on the slimes at pH 4.5. The final nickel recovery was 38.1% for nickel at a grade of 0.13%. This flotation recovery would represent an extra 4% nickel recovery when adjusted to the circuit feed stream. This result aligns well with the difference observed in the nickel recovery between the whole sample (64.7%) and the deslimed sample (61.3%) (See Table 4). A similar analysis for sulfur recovery to the one presented here for nickel recovery is available in the Supplementary Material.

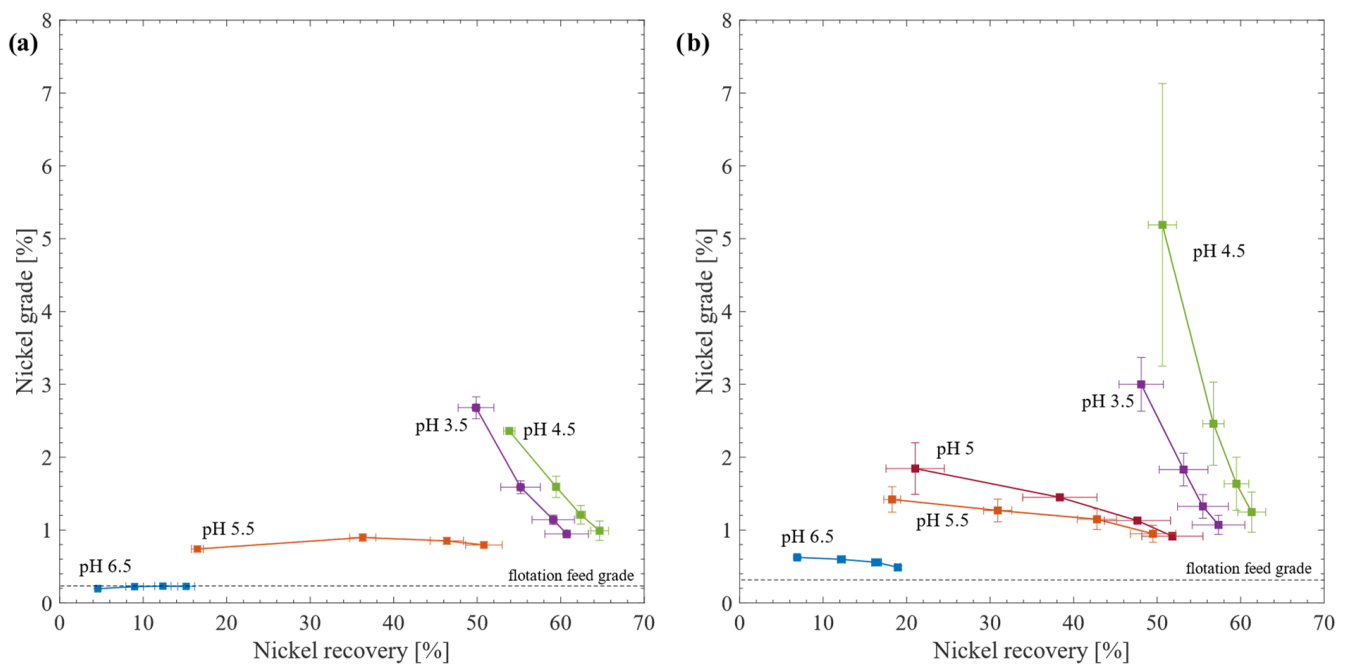


Figure 2. Nickel grade vs. recovery at different pH values: (a) whole sample, (b) deslimed sample. Error bars represent one standard deviation based on duplicate tests.

The flotation performance at pH 5 was evaluated for the deslimed sample to better discriminate the inflection point between pH 4.5 and 5.5. The results showed that nickel grades and recoveries at pH 5 are similar to values obtained for pH 5.5, such that the inflection point with respect to flotation is within the pH 4.5 to 5 range (Table 4). The identification of the higher pH level for an efficient nickel flotation is important since the lower the pH level, the higher the acid consumption, which translates into higher processing costs.

The effect of the acidic conditions on the awaruite flotation has been discussed in a previous microflotation study by the same authors [21]. The results of single mineral experiments and voltammograms showed that the surface of awaruite is activated in weakly acidic conditions (buffer pH 4.6) by the dissolution of the passivation layer that forms under neutral and alkaline conditions. The passivation layer formed in neutral and alkaline solutions was shown to inhibit the interaction between xanthate and the awaruite surface. The mechanism proposed to explain how xanthate (X^-) interacts with awaruite to induce hydrophobicity is that xanthate chemisorbs onto awaruite (X_{ads}) (Equation (1)) and then it oxidizes to form dixanthogen ($X_2(l)$) (Equation (2)). The chemisorption of xanthate leads to the formation of nickel xanthate on the active sites. The chemisorption can be seen as an intermediate reaction on the oxidation of xanthate, where the adsorbed xanthate species further oxidize into dixanthogen [21].



The results of the bench flotation tests conducted in the present study confirm that similar results can be achieved at a larger scale in the presence of serpentine and other gangue minerals.

The passivation layer on the awaruite surface is likely formed during grinding since the natural pH of the Baptiste ground sample is about 9.8 (Figure 3). The alkalinity of the sample is mainly linked with the presence of brucite in the rock, as a mineral produced in the serpentinization process. The passivation layer in nickel-iron alloys of similar

composition to the awaruite composition has been shown to have a thickness of 1 to 2.5 nm at pH 9.2 [26]. The passive film consists mainly of nickel oxide, NiO, and readily dissolves in acidic conditions [27]. Electrochemical studies showed that 10 min of conditioning was sufficient to completely dissolve the passivation layer at pH 4.6 [21]. The pH conditioning used in this work of 10 min prior to the addition of the collector showed to be sufficient to have the same effect on the natural awaruite present in the rock. The presence of other minerals in the sample does not interfere with the activation of awaruite.

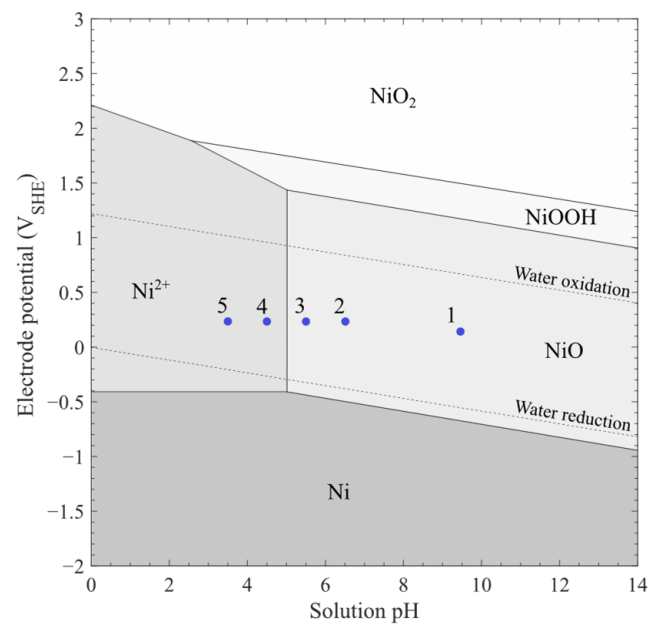


Figure 3. Eh-pH diagram for the Ni-water system ($[\text{Ni}^{2+}] = 10^{-6}$ mol/L, 298.15 K, 1 bar) adapted from [28]. Points: (1) natural pH, (2) pH 6.5, (3) pH 5.5, (4) pH 5.5 and (5) pH 3.5.

The NiO phase, which is the main component of the passivation layer, is thermodynamically stable in neutral and alkaline conditions, and the NiO-Ni²⁺ stability boundary resides at about pH 4.9 for the electrochemical potentials measured in the flotation cell [28]. The pH and potential measured in the flotation cell are shown with dots in Figure 3. Point 1 represents the natural slurry conditioning before the pH adjustment. The rest of the points, 2 to 5, represent the conditions after adjustment to pH 6.5, 5.5, 4.5, and 3.5, respectively. The stability boundary for the NiO-Ni²⁺ couple resides in between points 3 and 4, which correspond to the pH 5.5 and 4.5. The change observed in the results obtained at these two pH levels aligns well with the reported phase diagram for the nickel-water system, thus supporting the passivation layer as the main reason behind the poor flotation performance of awaruite in neutral and alkaline conditions. Even though the stability lines shown in the phase diagram are in equilibrium conditions, they serve as an indication of the phase that is more likely to be found in each condition. The flotation tests take place in a few minutes, a period that may not be sufficient to achieve equilibrium conditions. However, in this case, the passivation is a process that only occurs on the surface and within a few atomic layers on the awaruite surface. Thus, the removal of the passivation layer can be considered a fast process in which, the equilibrium conditions may not be far from reach.

3.2.2. Acid Consumption

The overall acid consumption for each flotation condition is presented in Figure 4. The acid consumption considerably increases with decreasing pH levels. The Baptiste sample contains acid soluble, or partially soluble minerals including brucite (reaction (3)), calcium

and magnesium carbonates (reaction (4)), and serpentine (reaction (5)). The dissolution reactions of these minerals can be expressed as follows:

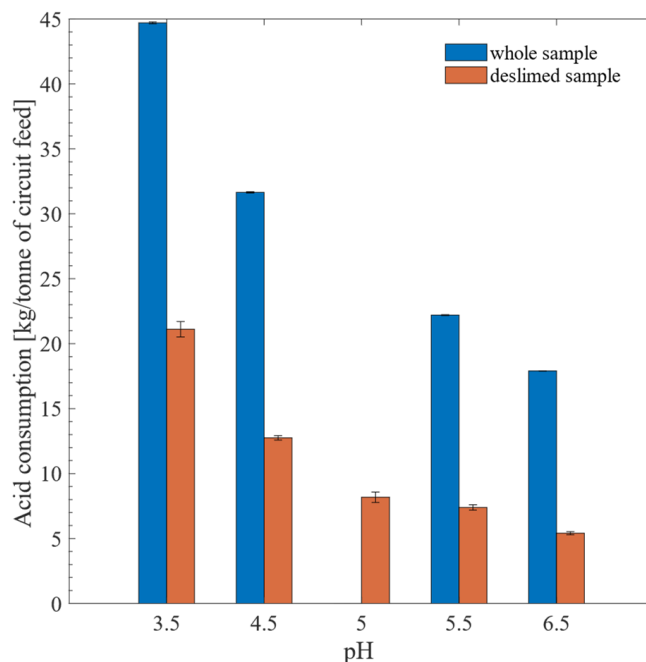
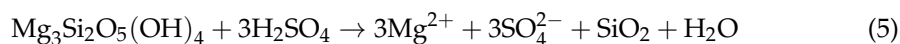
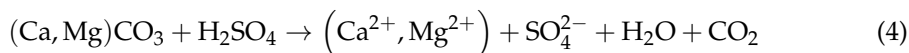


Figure 4. Overall acid consumption during flotation per ton of circuit feed at the different pH conditions for whole and deslimed samples.

It is expected that the brucite and the carbonates dissolve faster than the rest of the minerals present in the sample. Even though the conditioning took place for only 10 min, and the whole flotation process in less than 40 min, it is very likely that the brucite will dissolve almost completely. Brucite readily dissolves in less than 2 h when exposed to slightly acidic conditions [29]. The acid consumption linked to the brucite dissolution will be roughly 10 kg/ton if complete dissolution is assumed, accounting for a brucite concentration in the sample of 0.5% (Table 2) and following the stoichiometry presented in reaction (3). Similar dissolution kinetics have been measured for carbonates in ultramafic samples [29]. Following the same calculation path for calcium carbonates (reaction (4)), the acid consumption associated with carbonates would be 4 kg/ton. The dissolution of calcium carbonates may lead to the precipitation of gypsum in the presence of sulfate anions in the solution. The results collected in this work suggest that there is no significant effect of this precipitation on the flotation performance.

The estimated values of acid consumption are of the same order of magnitude as the values reported in Figure 4. Similar consumptions are reported for serpentinite ores; for instance, measurements for the Hitura mine for rich-serpentinite ores reported an acid consumption of about 10 kg/ton of feed to flotation to lower the pH down to 6.5 from 8. Furthermore, the estimated values confirmed that the acid is not only consumed by the brucite or carbonates but also by the serpentine minerals. However, the actual consumption is 1 to 2 orders of magnitude lower than expected for a complete reaction of serpentine. Whole ore leaching experiments of serpentinite ores at room temperature and pressure showed acid consumption in the order of hundreds or thousands of kilograms of sulfuric

acid [30]. These acid consumptions aligned well with the theoretical stoichiometry described in reaction (5). Desliming the sample prior to flotation considerably reduced the acid consumption for the same pH condition. For example, at pH 4.5, the acid consumption of the whole sample (31.7 kg/ton) is 148% higher than the consumption of the deslimed sample (12.8 kg/ton). Acid consumption profiles are shown in the Supplementary Material.

The rougher flotation results suggest that the best conditions for the selective separation of awaruite are at pH 4.5. Even though the recoveries at pH 4.5 and 3.5 are not considerably different, the acid consumption is lower for pH 4.5, which results in a more attractive option from a cost perspective. Regarding the decision to include the desliming or not, a detailed economic assessment has to be done, taking into account the difference in nickel recoveries and acid consumption. The results show that an extra 3% nickel recovery can be achieved by the flotation of the whole sample when compared to the deslimed sample; however, the acid consumption for the whole sample is more than twice the consumption of the deslimed sample.

3.3. Rougher-Cleaner Flotation

The results obtained in the rougher flotation assessment were further evaluated and complemented in a circuit including rougher and cleaner flotation. The nickel recoveries to the final concentrate in both cases were low when compared to the rougher flotation recoveries. For the whole sample, the nickel recovery to final concentrate was 31.1%, and for the deslimed sample, it was 26.8%. However, in these tests, the rougher nickel recoveries were similar to those obtained in the rougher flotation section for the same pH levels. For example, for the whole sample, the rougher recovery in this circuit was 64.8%, and in the rougher-only circuit, the recovery was 64.7%. The metallurgical balances for the whole, and deslimed samples are presented in the Supplementary Material, Tables S2 and S3, respectively. The difference between the nickel recovery to the rougher and final concentrate is mainly explained by losses in the cleaner stages. Only one cleaner test was carried out for each sample; thus, the conditions are far from optimized. More testing is required to optimize the cleaning stages, mainly by implementing locked-cycle flotation tests [31]. However, these rougher-cleaner tests provide an indication of the potential to produce a high-grade saleable concentrate.

The results of the multielement analysis of the final concentrates are shown in Table 5. The nickel grade of the final concentrates obtained for both samples is considerably higher than the nickel grade expected for a typical nickel sulfide operation, with flotation as the main separation method. The nickel content of sulfide concentrates is reported to range from 5% to 15%, with an average grade of 10% [32–34]. For the Baptiste sample, the nickel grade of the concentrates was 45.2% and 39.5% for the whole and deslimed samples, respectively. The high nickel grade of the concentrates has implications on its downstream processing; in this case, the cost of concentrate treatment is expected to be lower than the cost of treatment for a sulfide concentrate. A less energy and carbon intensity process would be required to refine the concentrate. Furthermore, studies have shown that the Baptiste deposit has the potential to become a carbon neutral or negative operation because of the carbon sequestration capacity of the magnesium silicates and hydroxide minerals present in the rock. These minerals react with atmospheric CO₂ through weathering processes to form stable carbonate minerals [35,36].

In terms of refining options, it has been shown that awaruite readily dissolves in acid in mild conditions; metallurgical studies have shown good nickel extraction rates in pressure leach tests at 150 °C and 750 kPa [4]. The flotation concentrate has the potential to be considered for the manufacture of Class 1 nickel products, including nickel sulfate for electric vehicle batteries, in a similar way to the current approach for such products from nickel sulfide deposits. Furthermore, if needed, the concentrate could be separated into two streams using magnetic separation. This separation would allow us to produce a concentrate for stainless steel production with low sulfur and another concentrate with nickel sulfides to be used on the production of Class 1 products.

Table 5. Elemental composition of rougher-cleaner concentrates for the whole and deslimed samples as obtained by multi-element analysis.

Element	Ni [%]	Fe [%]	Mg [%]	S [%]	Co [%]	Cu [%]
Whole sample concentrate	45.2	16.1	8.02	3.13	1.03	0.52
Deslimed sample concentrate	39.5	15.7	8.41	5.72	1.34	0.69
Element	Al [ppm]	Ca [ppm]	Cr [ppm]	Zn [ppm]	Mn [ppm]	Ti [ppm]
Whole sample concentrate	3140	1510	652	254	254	97
Deslimed sample concentrate	2720	1870	771	665	297	146
Element	As [ppm]	Cd [ppm]	Hg [ppm]	Pb [ppm]	Sb [ppm]	Se [ppm]
Whole sample concentrate	82	<2	<0.3	<200	<60	<30
Deslimed sample concentrate	170	<2	<0.3	<200	<60	<30

The minimum theoretical cobalt and copper grades to be considered in the concentrate payment for sulfide operations are 0.5% for cobalt and 0.4% for copper [32]. Both cobalt and copper contents are relevant since their values are higher than the theoretical minimum, and they could generate an extra return. Currently, these two elements are not included in the mineral resource estimation of the Baptiste deposit. However, the flotation results show that an extra return may be generated without the addition of any other separation.

Usually, a concentrate purchase contract specifies not only minimum nickel, cobalt, and copper content but also maximum levels of deleterious elements such as magnesium, arsenic, mercury, lead, selenium, cadmium, and antimony. For example, an arsenic concentration of 400 ppm is considered the maximum acceptable value for nickel sulfide concentrates, and penalties are applied when the concentrations are higher than 200 ppm. The arsenic contents shown in Table 5 are below 200 ppm; thus, no deduction would be applied to a Baptiste concentrate. Furthermore, the concentrations of cadmium, mercury, lead, and antimony are low, which would contribute to considering the concentrates as high-quality concentrates. The concentrates reported about 8% of magnesium content, but the theoretical maximum limit for a sulfide concentrate is 4% to 5%. More flotation steps or finer grinding would be required to reduce the magnesium content to even lower values to improve the quality of the concentrate in terms of magnesium content.

4. Conclusions

As a nickel-bearing mineral with high nickel content, awaruite represents a promising source of nickel for not only stainless-steel production but also for clean energy technologies. Awaruite was selectively floated under weakly acidic conditions using a xanthate collector. This is the first comprehensive research study to confirm that awaruite can be selectively floated in acidic conditions at bench scale. Nickel recoveries of up to 65% in rougher stages were obtained from a ground sample of the Baptiste deposit. The pH adjustment to values below 4.5 was critical to obtain good nickel recoveries. Desliming was shown to be an effective operation to considerably reduce the acid consumption in the flotation process. Nickel sulfides, present in the sample in a minor quantity compared to awaruite, were also recovered to the flotation concentrate. The final flotation concentrates from the Baptiste sample showed unique characteristics in terms of the high nickel content and negligible presence of penalty elements. The continuing development of clean energy technologies requires a shift into sustainable sources of metals, where nickel production from awaruite deposits could play an important role.

Supplementary Materials: The following supporting information can be downloaded at: <https://www.mdpi.com/article/10.3390/min13091147/s1> ([37–41]), Figure S1: Photo of Mozley C125 two-inch (5.1 cm) stub hydrocyclone mounted in a standard Mozley test rig; Figure S2: Bench scale set-up including the pH-Eh control system and the flotation cell; Figure S3: (a) Particle size distribution of the Baptiste sample after 15 min grinding (feed to the desliming process), and of the underflow and overflow of the desliming process; (b) corrected and uncorrected partition curves for the hydrocyclone desliming tests; Figure S4: Sulfur grade vs. recovery at different pH values: (a) whole sample, (b) deslimed sample. Error bars represent one standard deviation based on duplicate tests; Figure S5: Time profiles of pH and acid consumption for the whole and deslimed sample, and the slimes. The different stages during the flotation process are shown next to the *x*-axis, the time associated to each conc (Conc. #) includes collector and frother conditioning (3 min) and concentrate collection (2 min); Table S1: Operating parameters for the hydrocyclone desliming tests; Table S2: Metallurgical balance of the rougher-cleaner circuit for the whole sample.

Author Contributions: Conceptualization, S.S., G.S., M.P. and B.K.; Data curation, S.S. and M.P.; Formal analysis, S.S.; Funding acquisition, P.B. and B.K.; Investigation, S.S.; Methodology, S.S.; Project administration, B.K.; Resources, P.B. and B.K.; Software, S.S.; Validation, S.S.; Visualization, S.S.; Writing—original draft, S.S.; Writing—review and editing, S.S., G.S., M.P., P.B. and B.K. All authors have read and agreed to the published version of the manuscript.

Funding: The authors would like to thank Mitacs and FPX Nickel Corporation under the Accelerate Program (IT13501) for supporting this research project. The International Doctoral Fellowship from the University of British Columbia is also acknowledged for providing funding for Santiago Seiler. Santiago Seiler also acknowledges funding from Universidad de la República, Uruguay.

Data Availability Statement: The data presented in this study are available on request from the corresponding author. The data are not publicly available due to confidentiality restrictions.

Conflicts of Interest: The authors declare no conflict of interest.

References

1. IEA. The Role of Critical Minerals in Clean Energy Transitions. 2021. Available online: <https://www.iea.org/reports/the-role-of-critical-minerals-in-clean-energy-transitions> (accessed on 10 December 2021).
2. Mudd, G.M. Global trends and environmental issues in nickel mining: Sulfides versus laterites. *Ore Geol. Rev.* **2010**, *38*, 9–26. [CrossRef]
3. Norgate, T.; Jahanshahi, S. Assessing the energy and greenhouse gas footprints of nickel laterite processing. *Miner. Eng.* **2011**, *24*, 698–707. [CrossRef]
4. Grandillo, A.; Voordouw, R.; Simpson, R.; Chen, G.; Ennis, S.; Austin, J. NI 43-101 Technical Report-Preliminary Economic Assessment-Baptiste Nickel Project. In *FPX Nickel Corporation*; SGS Canada, Inc.: Vancouver, BC, Canada, 2020.
5. Ulrich, G.H.F. On the discovery mode of occurrence, and distribution of nickel-iron alloy awaruite on the west coast of South Island, New Zealand. *Q. J. Geol. Soc.* **1890**, *46*, 619–633. [CrossRef]
6. Seiler, S.; Sánchez, G.; Bradshaw, P.; Klein, B. Awaruite, a new large nickel resource. Part 1: Physicochemical properties and their implication for mineral processing. *Miner. Eng.* **2022**, *186*, 107754. [CrossRef]
7. Britten, R. Regional Metallogeny and Genesis of a New Deposit Type-Disseminated Awaruite (Ni₃Fe) Mineralization Hosted in the Cache Creek Terrane. *Econ. Geol.* **2017**, *112*, 517–550. [CrossRef]
8. Steinthorsdottir, K.; Cutts, J.; Dipple, G.; Milidragovic, D.; Jones, F. Origin and serpentinization of ultramafic rocks in dismembered ophiolite north of Trembleur Lake, central British Columbia. *Geol. Fieldwork* **2020**, *1*, 49–58.
9. Klein, C.; Hurlbut, C.S.; Dana, J.D. *Manual of Mineralogy (after James D. Dana)*; John Wiley & Sons, Inc.: New York, NY, USA, 1993; pp. 334–371.
10. White, G.N.; Dixon, J.B. Kaolin-serpentine minerals. In *Soil Mineralogy with Environmental Applications*; Soil Science Society of America: Madison, WI, USA, 2002; Volume 7, pp. 398–414. [CrossRef]
11. Edwards, C.; Kipkie, W.; Agar, G. The effect of slime coatings of the serpentine minerals, chrysotile and lizardite, on pentlandite flotation. *Int. J. Miner. Process.* **1980**, *7*, 33–42. [CrossRef]
12. Senior, G.; Thomas, S. Development and implementation of a new flowsheet for the flotation of a low grade nickel ore. *Int. J. Miner. Process.* **2005**, *78*, 49–61. [CrossRef]
13. George, C. The Mt Keith Operation. In *Nickel '96, Kalgoorlie*; AusIMM: Carlton, VIC, Australia, 1996.
14. Dai, Z.; Bos, J.A.; Quinn, P.; Lee, A.; Xu, M. Flowsheet development for Thompson ultramafic low-grade nickel ores. In Proceedings of the 48th Annual Conference of Metallurgists of CIM, Sudbury, ON, Canada, 23–26 August 2009.
15. Nasrallah, K.; Muinonen, J. Geometallurgical modeling of the Dumont Deposit. In Proceedings of the 48th Annual Canadian Mineral Processors Operators Conference, Ottawa, ON, Canada, 19–21 January 2016.

16. Uddin, S.; Rao, S.; Mirnezami, M.; Finch, J. Processing an ultramafic ore using fiber disintegration by acid attack. *Int. J. Miner. Process.* **2012**, *102*, 38–44. [[CrossRef](#)]
17. Fowler, R.P. Electrolytic Process and Apparatus for Recovering Nickel from Asbestos Ore. U.S. Patent US3677919A, 18 July 1972.
18. Fowler, R.P. Separation of Nickel from Asbestos Ore. U.S. Patent US3645454A, 29 February 1972.
19. Fischmann, A.J.; Dixon, D.G. Awaruite (Ni₃Fe) as a nickel resource—Leaching with ammoniacal–ammonium solution containing citrate and thiosulfate. *Hydrometallurgy* **2009**, *99*, 214–224. [[CrossRef](#)]
20. Seiler, S.; Sánchez, G.; Bradshaw, P.; Klein, B. Awaruite, a new large nickel resource. Part 2: Assessment of magnetic separation. *Miner. Eng.* **2023**, *191*, 107966. [[CrossRef](#)]
21. Seiler, S.; Sánchez, G.; Teliz, E.; Díaz, V.; Bradshaw, P.; Klein, B. Awaruite, a new large nickel resource: Electrochemical characterization and surface composition under flotation-related conditions. *Miner. Eng.* **2022**, *184*, 107656. [[CrossRef](#)]
22. Iwasaki, I.; Cooke, S.R. The decomposition of xanthate in acid solution. *J. Am. Chem. Soc.* **1958**, *80*, 285–288. [[CrossRef](#)]
23. Gupta, A.; Yan, D.S. Chapter 12—Classification. In *Mineral Processing Design and Operation. An Introduction*; Elsevier: Amsterdam, The Netherlands, 2006; pp. 354–400. [[CrossRef](#)]
24. Jobin-Bevans, S.; Siriunas, J. *Independent Technical Report on the Crawford Nickel-Cobalt Sulphide Project*; Caracle Creek International Consulting Inc.: Sudbury, ON, Canada, 2020.
25. Steinhorsdottir, K. Formation and Preservation of Brucite and Awaruite in a Serpentinized Ultramafite, Central British Columbia: Implications for Carbon Sequestration and Nickel Recovery. Master’s Thesis, The University of British Columbia, Vancouver, BC, Canada, 2021. [[CrossRef](#)]
26. Basile, F.; Bergner, J.; Bombart, C.; Rondot, B.; Le Guevel, P.; Lorang, G. Electrochemical and analytical (XPS and AES) study of passive layers formed on Fe–Ni alloys in borate solutions. *Surf. Interface Anal.* **2000**, *30*, 154–157. [[CrossRef](#)]
27. Marcus, P.; Olefjord, I. ESCA Studies of Ni-25 At% Fe Alloy 2-Dissolution and Passivation. *Surf. Interface Anal.* **1982**, *4*, 29–33. [[CrossRef](#)]
28. Huang, L.F.; Hutchison, M.J.; Santucci, R.J.; Scully, J.R.; Rondinelli, J.M. Improved Electrochemical Phase Diagrams from Theory and Experiments: The Ni-Water system and Its Complex Compounds. *J. Phys. Chem. C* **2017**, *121*, 9782–9789. [[CrossRef](#)]
29. Jowett, L. The Influence of pH and Dispersants on Pentlandite-Lizardite Interactions and Flotation Selectivity. Master’s Thesis, University of South Australia, Adelaide, Australia, 1999.
30. McDonald, R.G.; Whittington, B.I. Atmospheric acid leaching of nickel laterites review. Part I. Sulphuric acid technologies. *Hydrometallurgy* **2008**, *91*, 35–55. [[CrossRef](#)]
31. Nishimura, S.; Hirose, H.; Shobu, K.; Jinnai, K. Analytical Evaluation of Locked Cycle Flotation Tests. *Int. J. O Miner. Process.* **1989**, *27*, 39–50. [[CrossRef](#)]
32. Selby, M.; White, D.T. Commodity Marketing—Nickel. In *Cost Estimation Handbook*; AusIMM: Carlton, Australia, 2011; pp. 502–507.
33. Crundwell, F.K.; Moats, M.S.; Ramachandran, V.; Robinson, T.G.; Davenport, W.G. *Extractive Metallurgy of Nickel, Cobalt and Platinum-Group Metals*; Elsevier: Amsterdam, The Netherlands, 2011. [[CrossRef](#)]
34. Warner, A.E.M.; Díaz, C.M.; Dalvi, A.D.; Mackey, P.J.; Tarasoy, A.V.; Jones, R.T. JOM world nonferrous smelter survey Part IV: Nickel: Sulfide. *JOM* **2007**, *59*, 58–72. [[CrossRef](#)]
35. Power, I.M.; Dipple, G.M.; Bradshaw, P.; Harrison, A.L. Prospects for CO₂ mineralization and enhanced weathering of ultramafic mine tailings from the Baptiste nickel deposit in British Columbia, Canada. *Int. J. Greenh. Gas. Control* **2020**, *94*, 102895. [[CrossRef](#)]
36. Lu, X.; Carroll, K.J.; Turvey, C.C.; Dipple, G.M. Rate and capacity of cation release from ultramafic mine tailings for carbon capture and storage. *Appl. Geochem.* **2022**, *140*, 105285. [[CrossRef](#)]
37. Asante, G. Adsorption of Dextrin ONTO sulphide Minerals and ITS effect on the Differential Flotation of the Inco Matte. Ph.D. Thesis, The University of British Columbia, Vancouver, BC, Canada, 1993. [[CrossRef](#)]
38. Miettunen, H.; Heiskanen, K.; Keiski, R.L. A few aspects of the connections between ore mineralogy and flotation results at Hitura nickel mine in Finland. *Mineral. Miner. Metall. Process.* **2015**, *32*, 38–44. [[CrossRef](#)]
39. Heiskanen, K.; Kirjavainen, V.; Laapas, H. Possibilities of collectorless flotation in the treatment of pentlandite ores. *Int. J. Miner. Process.* **1991**, *33*, 263–274. [[CrossRef](#)]
40. Liu, C.; Zhang, W.; Song, W.; Li, H. Effects of lizardite on pentlandite flotation at different pH: Implications for the role of particle-particle interaction. *Miner. Eng.* **2019**, *132*, 8–13. [[CrossRef](#)]
41. Tang, X.; Chen, Y. Using oxalic acid to eliminate the slime coatings of serpentine in pyrite flotation. *Miner. Eng.* **2020**, *149*, 106228. [[CrossRef](#)]

Disclaimer/Publisher’s Note: The statements, opinions and data contained in all publications are solely those of the individual author(s) and contributor(s) and not of MDPI and/or the editor(s). MDPI and/or the editor(s) disclaim responsibility for any injury to people or property resulting from any ideas, methods, instructions or products referred to in the content.